Accepted to *ApJ*

HST/STIS Spectroscopy of the White Dwarfs in the Short-Period Dwarf Novae LL And and EF Peg[1]

Steve B. Howell

Astrophysics Group, Planetary Science Institute, Tucson, AZ 85705

Boris T. Gänsicke

Department of Physics and Astronomy, University of Southampton, Southampton, SO17 1BJ, UK

Paula Szkody

Department of Astronomy, University of Washington, Seattle, WA 98195

Edward M. Sion

Villanova University, Villanova, PA 19085

ABSTRACT

We present new HST/STIS observations of the short-period dwarf novae LL And and EF Peg during deep quiescence. We fit stellar models to the UV spectra and use optical and IR observations to determine the physical parameters of the white dwarfs in the systems, the distances to the binaries, and the properties of the secondary stars. Both white dwarfs are relatively cool, having T_{eff} near 15000K, and consistent with a mass of $0.6M_{\odot}$. The white dwarf in LL And appears to be of solar abundance or slightly lower while that in EF Peg is near 0.1-0.3 solar. LL And is found to be 760 pc away while EF Peg is closer at 380 pc. EF Peg appears to have an ∼M5V secondary star, consistent with that expected for its orbital period, while the secondary object in LL And remains a mystery.

Subject headings: stars: individual (LL And, EF Peg) — stars: white dwarfs — cataclysmic variables — UV Spectroscopy

1. Introduction

Observations of the component stars within interacting binaries such as cataclysmic variables (CVs) are difficult as the collected flux is often contaminated, representing contributions from both of the component stars as well as accretion phenomena. We have undertaken a large HST program to obtain UV spectroscopy of the white dwarfs in a number of short-period dwarf novae. Our selection of short period CVs was made primarily on the basis of systems with low mass accretion rates (based on short-orbital period and outburst history) and actually detecting the white dwarf absorption wings in the optical spectra. Thus, UV spectroscopy was essentially guaranteed to provide data in which the white dwarf would contribute $\sim$90% of the UV continuum flux, allowing accurate modeling of its parameters. In addition to our ability to fit white dwarf models to the UV spectra, we can use the observations to set limits on the distance to the binary and as a fiducial point to construct multi-wavelength spectral energy distributions to be attempted.

In this paper, we report on our analysis of Hubble Space Telescope (HST)/Space Telescope Imaging Spectrograph (STIS) observations for the two short-period dwarf novae: LL And and EF Peg. LL And belongs to the class of short-period dwarf novae which have rare outbursts, only of the "super" variety, increasing in brightness by 6 magnitudes or more. Additionally, both systems have been suspected as CVs which may harbor very low mass, brown dwarf-like, secondary stars and be of extreme age. These properties have been used to define a small class of objects as Tremendous Outburst Amplitude Dwarf novae (TOADs; Howell, Szkody & Cannizzo 1995) of which the most famous member is WZ Sge. EF Peg is suspected as being a TOAD due to its large outburst amplitude. However, its inter-superoutburst time scale is not well known and may be as short as $\lesssim$1 year and normal outbursts may also occur (Howell et al. 1993). If these outbursts characteristics are true, EF Peg is unlikely to be a TOAD.

LL And has an orbital period near 78 minutes based on superoutburst observations (Howell and Hurst 1994) with no radial velocity solution yet available. Optically, LL And is currently in a deep quiescent state with V$\sim$20 and with its last superoutburst being in 1993. Szkody et al. (2000) used an optical spectrum, which revealed the underlying white dwarf, and fit an 11,000K, 0.6 $M_{\odot}$ white dwarf model. Howell and Ciardi (2001) presented K-band spectroscopy of LL And which showed methane absorption indicating a very low

[1]Based on observations made with the NASA/ESA Hubble Space Telescope obtained at the Space Telescope Science Institute which is operated by the AURA under NASA contract NAS 5-26555 and with the Apache Point Observatory (APO) 3.5-m telescope which is operated by the Astrophysical Research Consortium (ARC).

effective temperature near 1300K. However, since Szkody et al. (2000) determined a lower limit to the distance for LL And of 346 pc, it is difficult to reconcile the methane absorption as originating in a low mass brown dwarf-like secondary star.

EF Peg has a longer orbital period, 2.05 hours, based on superoutburst photometry (Howell et al. 1993) but has been poorly studied due to its faintness, V$\lesssim$18.5 at minimum and its positional location within 5" of a 12th magnitude star, long thought to be the variable (See Howell et al. 1993). EF Peg had its last superoutburst in 1997 and no previous optical spectrum for EF Peg exists. Howell et al. also present a crude distance estimate for EF Peg of ∼600 pc based on a normal dwarf novae M_V–P_{orb} relation (Warner 1995). If a TOAD, EF Peg would be the longest orbital period member and therefore may be one of the oldest CVs in the Galaxy (Howell, Rappaport and Politano 1997). Recent K-band spectroscopy of EF Peg has been presented in Littlefair et al. (1999) and these authors concluded that the secondary star must be later than (cooler than) ∼M5V.

Details of our motivations, the HST program in general, and previous results are presented in Gänsicke et al. (2001) and Szkody et al. (2002). Our new HST observations are discussed in §2, our model fitting and analysis is given in §3, and we summarize the results of this work in Section 4.

2. Observations

HST/STIS observations of LL And and EF Peg were obtained on 12 July 2000 UT and 18 June 2000 UT using the G140L and E140M gratings respectively with the 52 X 0.2" aperture. The UV spectra covered the range of 1150-1715 Å with an estimated velocity resolution of ∼300 km s^{-1}. The total exposure times were 75 min for LL And (2 consecutive HST orbits) and 115 min for EF Peg (3 consecutive HST orbits). The summed spectra covered 93% (LL And) and 95% (EF Peg) of their orbital periods but were not consecutive in phase coverage due to the sampling imparted by the HST observations. Since neither star has a radial velocity solution and thus no ephemeris, the binary phases of the individual HST observations are unknown. We will see below, that only the summed observations had sufficient S/N to use for our purposes. The mean HST/STIS spectra of LL And and EF Peg are shown in Fig 1a and 1b, respectively

The UV spectrum of LL And (Fig. 1a) shows the typical disk emission line at CIV (1550 Å). A number of weak absorption lines can be clearly discerned in the spectrum: the CI 1277-1280 Å multiplet, CI 1335 Å and SiII 1306, 1527 & 1530 Å(Fig. 5 below). A number of additional transitions are marginally identified near the noise level. These absorption lines

are almost certainly from the white dwarf as they are not significantly broadened by rotation (as the disk emission lines are) and the observed ionization/excitation exactly matches the derived white dwarf photospheric temperature which we derive below. It is possible, though unlikely, that a disk at a low enough inclination could produce these absorption lines but at the distances derived (see below) luminosity arguments strongly support the photosphere interpretation. The quality of the spectrum in the wavelength range near 1300Å is degraded due to the subtraction of the Geocoronal OI airglow. Residual Lyα airglow is visible in the broad white dwarf Lyman absorption. For EF Peg (Fig. 1b), we see emission due to CIV as well as NV and SiIII and IV. Narrow absorption lines of CI (1277Å), SiII (1260/65 Å), and CII (1335 Å) are also observed. Quasi-molecular hydrogen absorption troughs (H_2^+ at 1400Å and H_2 at 1600Å) are not obvious in either star being weak at these temperatures and probably filled in by SiIV disk emission and/or lost in the continuum noise.

The STIS data were obtained in the *time-tagged* mode and we made use of this information to examine the photometric behavior of these two stars during our HST observations. Excluding a small region near Lyα, we produced 10-30 sec time resolution UV light curves by summing the continuum flux. Neither star showed any significant modulation during our observations, consistent with the assumption that nearly all the UV continuum light is from the white dwarf and does not contain a significant accretion disk/hot spot contribution.

Neither star has any previous UV spectra but given the rarity of their superoutbursts (last superoutburst for LL And was in 1993 and for EF Peg in 1997) as well as the AAVSO and other watchdog groups who monitor the TOADs for such outbursts not reporting any activity during our HST observations, we conclude that our UV spectra were taken during deep quiescence. Additionally, we will see below that both stars are at or below their reported minimum V magnitudes.

Optical spectra for EF Peg (3 July 2000 UT: within one month of the HST observation) and LL And (5 December 2000 UT) were obtained using the Apache Point Observatory 3.5m telescope and Double Imaging Spectrograph with a 1.5 arcsec slit, giving ∼2.5Å resolution spectra in the regions from 4200-5000Å and 6300-7300Å.

LL And is a fairly faint target and was observed for 1200 sec at an airmass of 2.8. Light cirrus was present during the observation, so the fluxes are highly uncertain. Although of low S/N (especially in the blue), the spectra obtained are consistent with that presented in Szkody et al. (2000) and are shown in Figure 2a as we use them in §3.3. The 5000Å flux corresponds to an approximate V magnitude of ∼20.6, fainter than the V=19.9 value reported by Szkody et al. (2000) for LL And in 1996 when only 3 years past its last superoutburst. Given the high airmass of our observation and the cirrus present, we take these values as being consistent. The Szkody et al. spectrum of LL And showed the presence of underlying

WD absorption in Hβ and the higher Balmer lines, but we cannot conclusively detect the absorption in our poor quality blue spectrum. However, the optical spectra of LL And do show the presence of double-peaked emission lines for Hα and Hβ and a weak blue continuum of a dwarf novae at minimum. Both of these properties are indications of a system with low mass transfer and a mostly optically thin accretion disk (See Mason et al. 2000). Given the rare outbursts of this star, these properties are all typical signs of a quiescent state TOAD.

For EF Peg, 3x900 sec exposures were obtained over an airmass range of 1.6-1.9. The average spectrum is shown in Figure 2b and converting the flux at 5000 Å to an approximate visual magnitude gives V$\sim$19. Even though the observation was through a narrow slit and there were passing clouds during the night, we find that it is in good agreement with the published quiescent V magnitude for EF Peg (Howell et al. 1993). We see clear evidence for white dwarf absorption in EF Peg at Hβ and Hγ. Figure 2b also shows the typical double-peaked Balmer line profiles and weak blue continuum of a low mass transfer rate CV at minimum light.

3. Model Fitting and Analysis

Our white dwarf spectral analysis is carried out in two stages: in a first step, we derive the effective temperature $T_{\rm eff}$ and the surface gravity $\log g$ as well as a rough estimate of the chemical abundances in the atmosphere. In a second step, we refine the analysis of the abundances and determine the white dwarf rotation rate. All the model spectra used throughout this analysis are generated using TLUSTY195 and SYNSPEC45 (Hubeny 1988; Hubeny & Lanz 1995).

During the first stage, we calculate three different grids of model spectra covering $T_{\rm eff} = 10,000 - 25,000\,{\rm K}$ in steps of 100K and $\log g = 7.0 - 10.0$ in steps of 0.1, assuming 0.1, 0.5, and 1.0 times solar abundances. We fit the models to the HST/STIS data with the emission lines (presumably originating in the accretion disk) added in as simple Gaussian profiles in the fitting procedure and we exclude from the fit a 20Å wide region centered on Lyα.

In principle, one can determine from such model fits both the temperature and the $\log g$ independently as both parameters determine the detailed shape of the continuum and line profiles. However, in the case of LL And and EF Peg, this is difficult as the data have a relatively modest S/N and the Lyα absorption profile is contaminated with both disk and terrestrial emission, especially in the case of EF Peg. In order to test the correlation between $T_{\rm eff}$ and $\log g$, we keep $\log g$ fixed and determine the best-fit effective temperature, repeating this procedure for each individual $\log g$ in our model grid. We find that $T_{\rm eff}$ and $\log g$ are

approximately linearly correlated, with statistically insignificant differences in χ^2.

Using a Hamada-Salpeter mass-radius relation (Hamada & Salpeter 1961) for carbon-core white dwarfs[2] we compute from $\log g$ the white dwarf mass $M_{\rm WD}$ and its radius $R_{\rm WD}$. From the scaling factor ($\rm R^2_{WD}/d^2$) between the model spectrum and the observations (assuming negligible extinction for these high-galactic latitude objects), we obtain an estimate for the distances of the systems. Finally, we compute V magnitudes from the optical extensions of the model spectra used for the STIS analysis. Using our initial white dwarf model grid, we calculated χ^2 values (over the entire range of $\log g$) for both stars. For LL And, a minimum from $\log g$=7.2-8.1 was found with $\chi^2 \lesssim$1.1. For EF Peg, $\chi^2 \lesssim$2.8 over the minimum covering $\log g$=7.0-8.2. The parameters $M_{\rm WD}$, $T_{\rm eff}$, d, and V are shown as a functions of $\log g$ in Fig. 4 (LL And) and Fig. 7 (EF Peg). Over a fiducial range $\log g = 8.0 \pm 0.5$ (corresponding to $M_{\rm WD} = 0.33 - 0.90\,M_\odot$), we find $T_{\rm eff}$ to be constrained to $\pm$1000 K.

While the STIS data alone are insufficient to determine independently the temperature and the mass of the white dwarf, additional constraints can be obtained from combining the UV data with optical/IR coverage. The distance value determined critically depends on the assumed white dwarf radius but the use of equal (minimum) state, optical (and IR) observations help constrain it as well. Using our models over a range of $\log g$, we can assess their temperature dependence and thus their flux contribution to longer wavelength bandpasses. A lower limit to $\log g$ can be obtained by assuming that the optical flux can not lie below our white dwarf model. An absolute upper limit to $\log g$ is established by the theoretical upper mass limit (1.4 $\rm M_\odot$) for a white dwarf. We discuss these ideas further in §3.3 but note here that, when taken together, all the observed parameters favor a best choice for $\log g$=8.0 for both stars.

After having established ($\log g$, $T_{\rm eff}$) from the combined ultraviolet plus optical observations, we made the attempt to refine the models in terms of the chemical abundances and white dwarf rotation rates. We plotted our STIS data along with model spectra computed for 0.1, 0.5, and 1.0 times solar abundances, convolving each of these models with rotation rates of $v \sin i = 100 - 1200\,\rm km\,s^{-1}$. Considering the noise level of the data, we judged the goodness of the match between data and model by visual inspection rather than by a formal fit. Our experience is that at times, such formal fitting to data of this S/N can lead to false estimations of the best χ^2 fit.

---

[2]The use of the zero-temperature $M - R$ relation is justified for our purpose, as the increase in radius of finite-temperature white dwarfs is small in the temperature range considered here, and insignificant compared to other uncertainties.

3.1. LL And

Our HST spectrum of LL And is rather noisy due to the intrinsic faintness of this object and the short integration time, thus we co-added both HST orbits for our analysis. Using $\log g = 8.0 \pm 0.5$, which corresponds to a white dwarf mass of $0.6 \pm 0.3 M_{\odot}$, we find an effective temperature of $14,300 \pm 1000$ K and a distance of 760 ± 100 pc for LL And. This model is shown in Figure 3 and the dependence of our determined parameters on $\log g$ is presented in Figure 4. These model parameters predict a white dwarf only apparent magnitude of V=20.8, in good agreement with our minimum system V magnitude of near 20.6. Thus, we expect that at the present time the accretion disk contributes little flux to the (blue) optical bandpass; a result which agrees with our observation of no significant blue continuum rise (Figure 2a).

The moderate S/N of the STIS data prevents a detailed analysis of the abundance pattern, but our fits *suggest* slightly sub-solar abundances for the atmosphere of the white dwarf. While there are only a very limited number of metal absorption lines available that can be used to measure the rotation rate, we are confident that the white dwarf spin is significantly below Keplerian velocity; we estimate $v \sin i \lesssim 500\,\mathrm{km\,s^{-1}}$ (see Fig. 5) where it can be seen that a best match occurs for velocities below 500 $\mathrm{km\,s^{-1}}$.

3.2. EF Peg

Due to the moderate S/N in each of the three HST orbits of STIS spectra for EF Peg, we have summed the data together for our analysis presented here. Our model for EF Peg is shown in Figure 6 and the dependence of our determined parameters on $\log g$ is presented in Figure 7. We find a white dwarf mass of 0.6±0.3 $M_{\odot}$ ($\log g$=8.0±0.5). a WD temperature of 16,600±1000K, a distance of 380±60 pc, and a white dwarf only V magnitude of 19.1. Our "spectral" V magnitude of ∼19 again assures us of little accretion disk flux contamination in the (blue) optical bandpass, as seen in Fig. 2b as a lack of a rising blue continuum.

The determination of the elemental abundances present in EF Peg is *uncertain* due to the (unknown amount of) contamination of line emission in and near the absorption features, especially for the carbon and the silicon lines. The overall abundances appear to be sub-solar ($\sim 0.1 - 0.3\times$ solar). We have used these abundance estimates to provide an adequate fit (Fig. 6) to the UV spectra. Figure 8 shows the STIS data of EF Peg along with the white dwarf model just described convolved with rotation rates of $v\sin i$=100, 300, and 500 $\mathrm{km\,s^{-1}}$. Examination of the different absorption lines, in particular the SiII 1260/65 Å doublet, shows that the rotation rate of the white dwarf in EF Peg is very low, the best match is indeed

obtained for $v\sin i \lesssim 300$ km s^{-1}.

3.3. Spectral Energy Distributions and the Secondary Stars

In order to provide an additional constraint on the $\log g$ values determined in the UV fitting process, we can make use of the optical spectra obtained for LL And and EF Peg. Using the assumption that the "state" of the system was similar, the optical spectra set a limit on the WD flux as it cannot be higher than the value measured with any additional optical flux being due to accretion phenomena. We have also seen above that for both of these stars during the time of the optical observations, there is likely to be little contamination in the optical, particularly in the blue region, due to the accretion disk.

Figure 9 shows the spectral energy distribution (SED) for LL And based on our UV and optical spectroscopy. The UV models in the optical bandpass, show that the $\log g = 7.5$ model is unlikely as it would provide too much optical flux and the $\log g = 8.5$ model provides too little to the blue (uncontaminated) optical flux. Thus, a $\log g$=8.0 model is the most plausible fit for these data.

In Fig. 9, we also plot the K band magnitude obtained by Howell & Ciardi (2001) for LL And based on IR spectroscopy. Their low S/N spectrum revealed the presence of methane absorption in LL And and, if confirmed, would make the secondary star quite cool (T$\sim$1300K) and of very low mass ($\sim$0.04 M$_\odot$), in agreement with theoretical values if a post-period minimum CV. However, for such a secondary star the distance to LL And would need to be quite close, $\sim$30-60 pc, a result in severe disagreement with our value of 760 pc determined here and the lower limit of 346 pc determined by Szkody et al. (2000). The methane feature may possibly arise in the cool outer regions of the accretion disk while the true nature of the secondary star in LL And remains a mystery.

Figure 10 shows similar SEDs for EF Peg. The details of the models again provide a good constraint for our choice of a $\log g$=8.0 model as lower $\log g$ models would provide too much optical flux. In Fig. 10 we show the J and K magnitudes for EF Peg from Sproats et al. (1996). A check of the AAVSO records for EF Peg during the time of these observations (September 1993) reveals that the star was not in (super)outburst at the time of the IR observations.

Using the orbital period of EF Peg as a guide, we can estimate the expected parameters of its secondary star under the assumptions of it being either a pre- or a post-period minimum dwarf novae (Howell et al. 2001). For a pre-period minimum system, the secondary star should have T$\sim$2900K and a mass of $\sim$0.2 M$_\odot$, similar to the properties of a M5V star.

Using the two observed IR data points as an absolute scaling for a model fit (assuming zero disk contribution in the optical and IR) and taking a SED for a main sequence star, we can add into Fig. 10 the expected flux values at 6400Å and 7000Å and the expected SED shape (dashed line) for a Roche-lobe filling M5V star. We find that for this type of secondary, we would not expect to detect it in our red optical spectrum, as its flux would be far less than that of even the WD alone at 7000Å. Assuming that the IR flux is almost entirely due to this type of a secondary star, a distance of $\gtrsim$290±50 pc is derived. This independent distance estimate is in good agreement with our determination above (380±60 pc) based on our assumed WD models.

The IR points only provide an upper limit as the actual percentage of secondary star and disk contribution to the continuum longward of 7000Å is unknown. However, the secondary star is unlikely to be too much later than ∼M5V in order for the IR continuum shape to agree with observations. We note that a post-period minimum secondary star of extreme low temperature and mass would not be able to provide the observed IR fluxes unless the system was very nearby *or* the accretion disk dominates in the IR and has a spectral shape similar to an M star. However, both of these facts would make the WD contribution in the UV and optical very difficult to reconcile. Assuming the secondary star is similar to an M5V, EF Peg is not likely to be a TOAD.

Subtraction of the WD (and secondary star for EF Peg) models from our optical spectra reveal that for LL And there is not much remaining optical flux. This result is consistent with a system of very low mass transfer and containing an optically thin accretion disk (See Mason et al. 2000). For EF Peg, we find residual flux remains in the red spectrum with a poorly constrained slope of $F_\lambda \sim \lambda^{-3}$, possibly indicating that the outer disk is marginally optically thick or that there is a weak single blackbody-like source (hot spot?) contributing in this region (See Mason et. al. 2001).

4. Summary

Using white dwarf models, our HST UV spectra of the stars LL And and EF Peg, and the additional constraints imposed by optical and IR measurements, we find the following: the white dwarfs in both of these short-period dwarf novae are consistent with a mass of $0.6 M_\odot (\log g = 8.0)$ and show derived temperatures near 15,000K. Using the most plausible models, we estimate the distance to LL And as 760 pc and to EF Peg as 380 pc. This distance estimate for EF Peg is considerably less than that calculated by Howell et al. (1993) using "normal" dwarf novae ideas of the absolute magnitude of the accretion disk at maximum (Warner 1995). The failing of that method is not unexpected, as we have ample evidence

that the accretion disks in low mass transfer dwarf novae are not "normal" at minimum, thus they probably do not follow a normal M_V relation at maximum. UV spectroscopy is a very important technique for providing good distance estimates for faint, short period cataclysmic variables as the usual null detection of the secondary star can, at best, only provide a limit. The abundance determinations from this work are not well constrained but indicate that the white dwarf in LL And is near or slightly below solar while that in EF Peg is near 0.1-0.3 solar.

Given the orbital periods of LL And and EF Peg, our rotation rate estimates for the white dwarfs in these two stars are generally consistent with the range evident in short period sytems (Sion 1999, Gansicke et al. 2001, Szkody et al. 2002). The quality of the LL And UV spectroscopy precludes us from setting a strict limit.

If the duty cycle for short-period, low mass transfer rate dwarf novae in deep quiescence is long, observational searches for very faint (V>18), essentially cool white dwarfs with (weak) Balmer emission and *close*, very low mass (substellar?) companions in extremely short orbital periods will be a difficult project. IR observations will be extremely helpful, however current surveys, such as 2MASS, are not yet deep enough to provide JHK measurements for the faintest CVs and their brown dwarf-like secondaries. Such a challenging observational program may be required to truly test the existence of the large hypothesized population of TOADs.

The authors would like to thank the anonymous referee for their comments. This research was partially supported by NASA through grant GO-08103-97A from the Space Telescope Science Institute, which is operated by the Association of Universities for Research in Astronomy, Inc. under NASA contract NAS5-26555. Additional support was provided by NSF grant AST-98-10770 to SBH and NSF grant AST-99-01955 to ES. BTG is supported by a PPARC Advanced Fellowship.

REFERENCES

Gänsicke, B. T., Szkody, P., Sion, E. M., Hoard, D., Howell, S. B., Cheng, F. H., & Hubeny, I., 2001, A&A, 374, 656

Hamada, T. Salpeter, E. E., 1961, ApJ 134, 683

Howell, S. B., Schmidt, R., DeYoung, J. A., Fried, R., Schmeer, P., & Gritz, L., 1993, PASP, 105, 579

Howell, S. B., & Hurst, G., 1994, JBAA, 106, No. 1, p. 29

Howell, S. B., Szkody, P., & Cannizzo, J., 1995, ApJ, 439, 337

Howell, S. B., Rappaport, S. & Politano, M., 1997, MNRAS, 287, 929

Howell, S. B., Nelson, L., & Rappaport, S, 2001, ApJ, 550, 518

Howell, S. B., & Ciardi, D. R., 2001, ApJL, 550, L59

Littlefair, S. P., Dhillon, V. S., Howell, S. B., & Ciardi, D. R., 1999, MNRAS, 313, 117

Mason, E., Skidmore, W., Howell, S. B., & Mennickent, R., 2001, ApJ, 563, 361

Mason, E., Skidmore, W., Howell, S. B., Ciardi, D., Littlefair, S., & Dhillon, V., 2000 MNRAS, 318, 440

Sion, E., M., Long, K. S., Szkody, P., & Huang, M., 1994, ApJL, 430, L53

Sproats, L. N., Howell, S. B. and Mason, K. O., 1996, MNRAS, 282, 1211

Szkody, P., Desal, V., Burdullis, T., Hoard, D., Fried, R., Garnavich, P., & Gänsicke, B., 2000, ApJ, 540, 983

Szkody, P., Gänsicke, B., Sion, E.,& Howell, S. B., 2002, in *The Physics of Cataclysmic Variables and Related Objects*, B. Gänsicke, K. Beuermann, and K. Reinsch Eds., ASP Conf. Series, 261, 21

Warner, B., 1995, *Cataclysmic Variable Stars*, Cambridge University Press

Figure captions

Figure 1: (a) Total STIS spectrum of LL And binned by 0.6Åand smoothed with a 3-point running boxcar. The bottom curve shows the 1σ statistical error of the *unsmoothed* data. Note the presence of CIV emission and the narrow geocoronal Lyα emission sitting in the broad white dwarf Lyα absorption. Some narrow white dwarf absorption lines are apparent, see text for details. (b) Total STIS spectrum of EF Peg binned by 0.6Å. The bottom curve shows the 1σ statistical errors, the wavelength-dependence of the error over the individual echelle orders can be seen in the sawtooth-like structure. Note the presence of CII-IV, and NV emission and the narrow geocoronal Lyα emission sitting in the broad white dwarf Lyα absorption. Some narrow white dwarf absorption lines are apparent, see text for details.

Figure 2: (a) Red and blue optical spectra for LL And obtained at APO. The blue channel is poor quality due to the faintness of the source, but the double-peaked nature of Hα and Hβ are apparent. The y axis is Flux in units of ergs cm^{-2}s^{-1}Å^{-1}. (b) Red and blue optical spectra for EF Peg obtained at APO. The double peaked structure of the Balmer emission lines is apparent as well as the broader underlying white dwarf absorption features in Hβ and Hγ. The y axis is Flux in units of ergs cm^{-2}s^{-1}Å^{-1}.

Figure 3: Our white dwarf model (thick line) compared with the LL And STIS data. The model has T=14,300K, M_{WD}=0.6 $M_\odot$ ($\log g$=8.0), and the abundances listed in Table 1. The Gaussians (dotted lines) represent our simple fits to the emission lines.

Figure 4: Our parameter plot for LL And showing the fitting parameters for M_{WD}, temperature, distance, and white dwarf V magnitude as a function of $\log g$.

Figure 5: Three rotation models for LL And all with v sin i=300 km s^{-1} with three different values of the abundance; 0.1, 0.3, and 1.0 times solar. We see that while none of the abundance models fit perfectly, a solar abundance model is reasonable. Useful photospheric absorption lines are marked.

Table 1. Summary of White Dwarf Model Fits

Star	T_{eff} (K)	$\log g$ (cm s^{-2})	Mass ($M_\odot$)	D (pc)	V_{WD} (Mag)	Abundance $\odot$	$v\sin i$ (km s^{-1})
LL And	14300±1000	8.0±0.5	0.6±0.3	760±100	20.8	$\lesssim$1.0	$\lesssim$500
EF Peg	16600±1000	8.0±0.5	0.6±0.3	380±60	19.1	0.1-0.3	$\lesssim$300

Figure 6: Our white dwarf model (thick line) compared with the EF Peg STIS data. The model has T=16,600K, M_{WD}=0.6 $M_{\odot}$ ($\log g$=8.0), and the abundances listed in Table 1. The Gaussians (dotted lines) represent our simple fits to the emission lines.

Figure 7: Our parameter plot for EF Peg showing the fitting parameters for M_{WD}, temperature, distance, and white dwarf V magnitude as a function of $\log g$.

Figure 8: Three rotation models for EF Peg with 0.1 solar metal abundances. The 100 km s^{-1} model appears to be the best fit. Useful photospheric absorption lines are marked.

Figure 9: SED model for LL And using HST/UV and APO/optical spectra. The three white dwarf models shown cover the range of interest. The single point at 22000 Å is the K band flux from Howell & Ciardi (2001). The spectra have been smoothed as we are concerned here with a broad band comparison.

Figure 10: SED model for EF Peg using HST/UV and APO/optical spectra. The three white dwarf models shown cover the range of interest. The points at 12200 and 22000 Å are the J and K band fluxes from Sproats et al. (1996). The dashed curve and the points at 6400 & 7000 Å are a M5V model SED scaled to the J and K fluxes. See text for details. The spectra have been smoothed as we are concerned here with a broad band comparison.

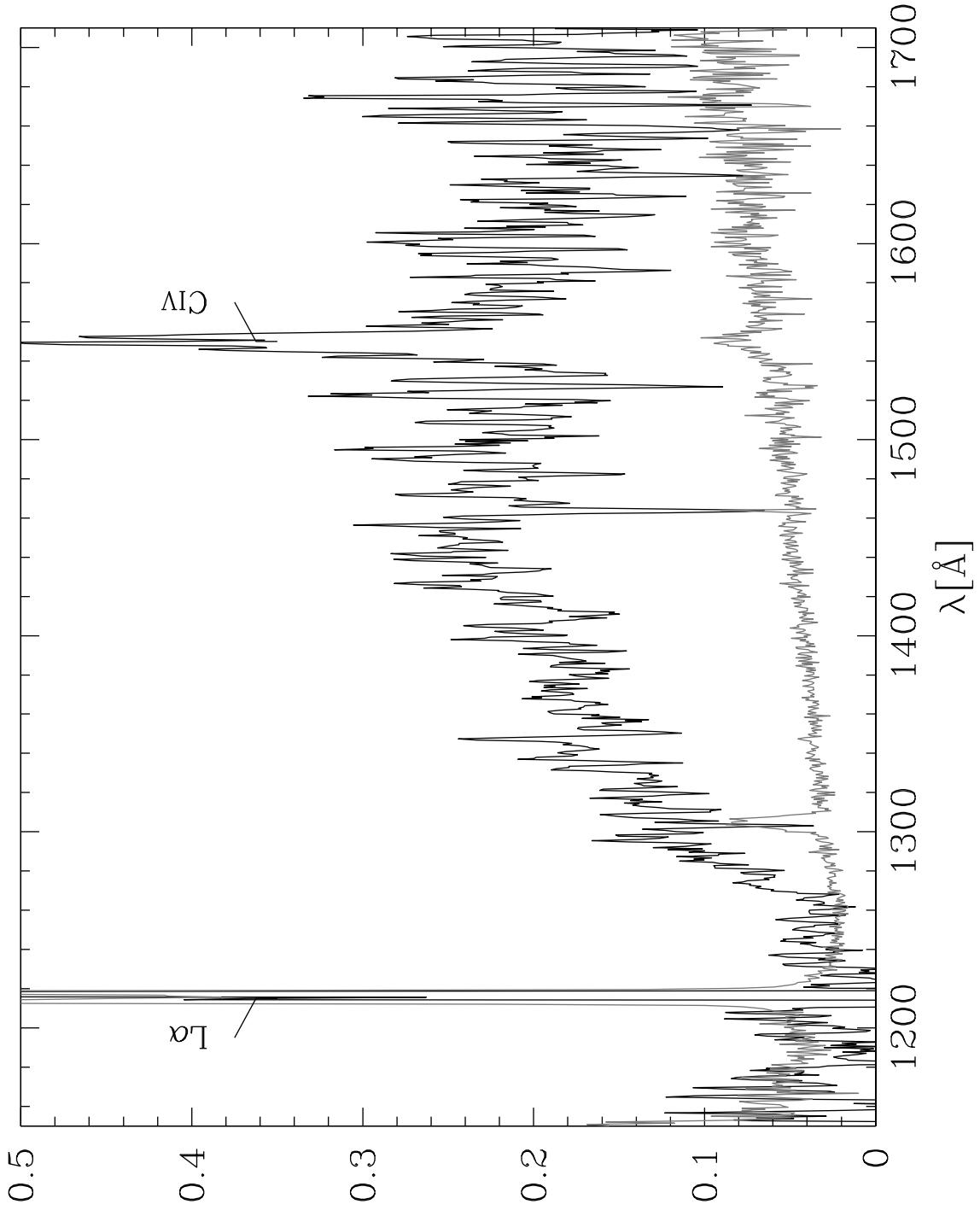
Lα
CIV
0
0.1
0.2
0.3
0.4
0.5
1200
1300
1400
1500
1600
1700
λ[Å]
F_λ [10^{-15}erg cm^{-2}s^{-1}Å^{-1}]

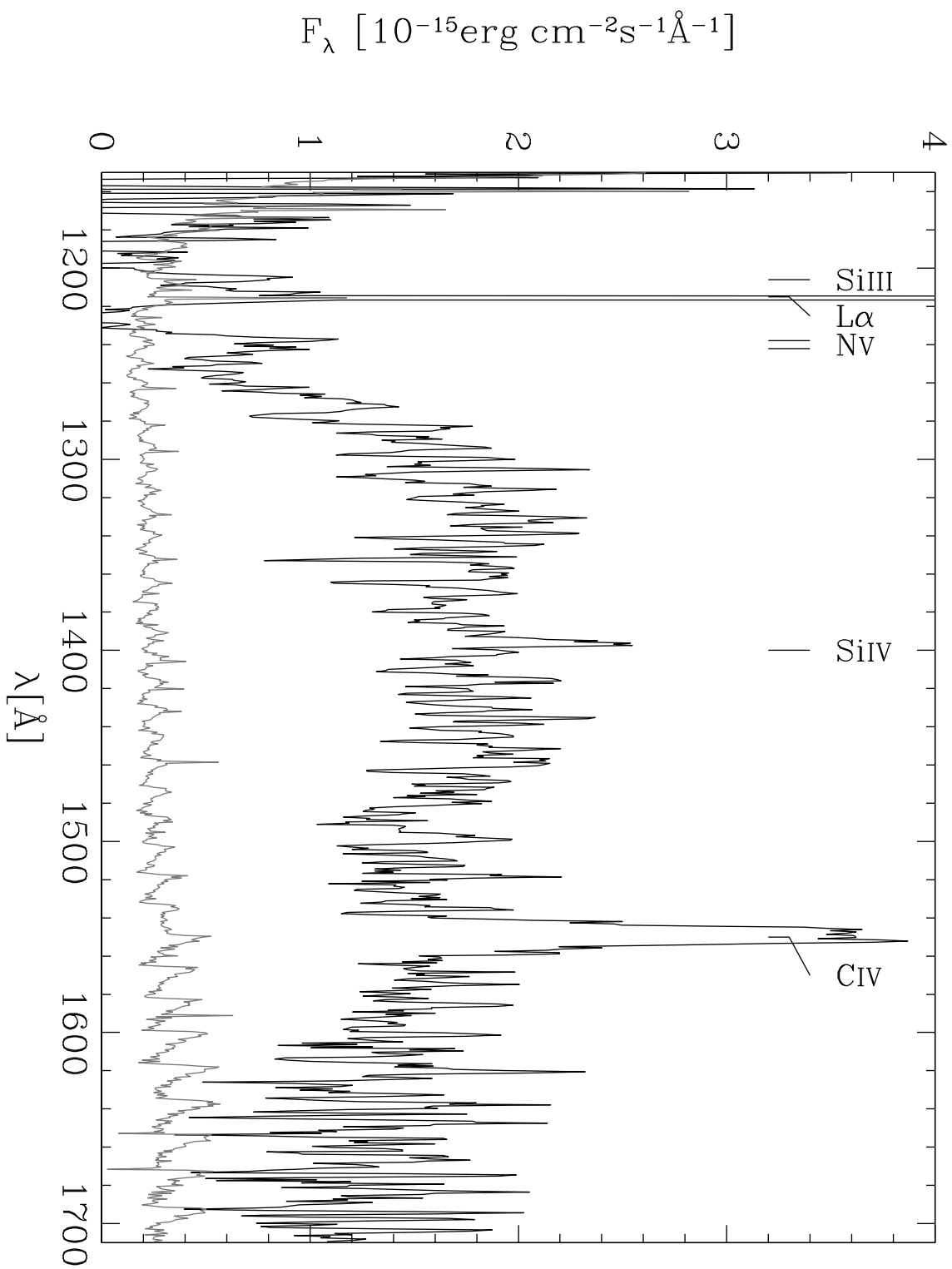
F_λ [10^{-15}erg cm^{-2}s^{-1}Å^{-1}]
0
1
2
3
4
1200
1300
1400
1500
1600
1700
λ[Å]
SiIII
Lα
NV
SiIV
CIV

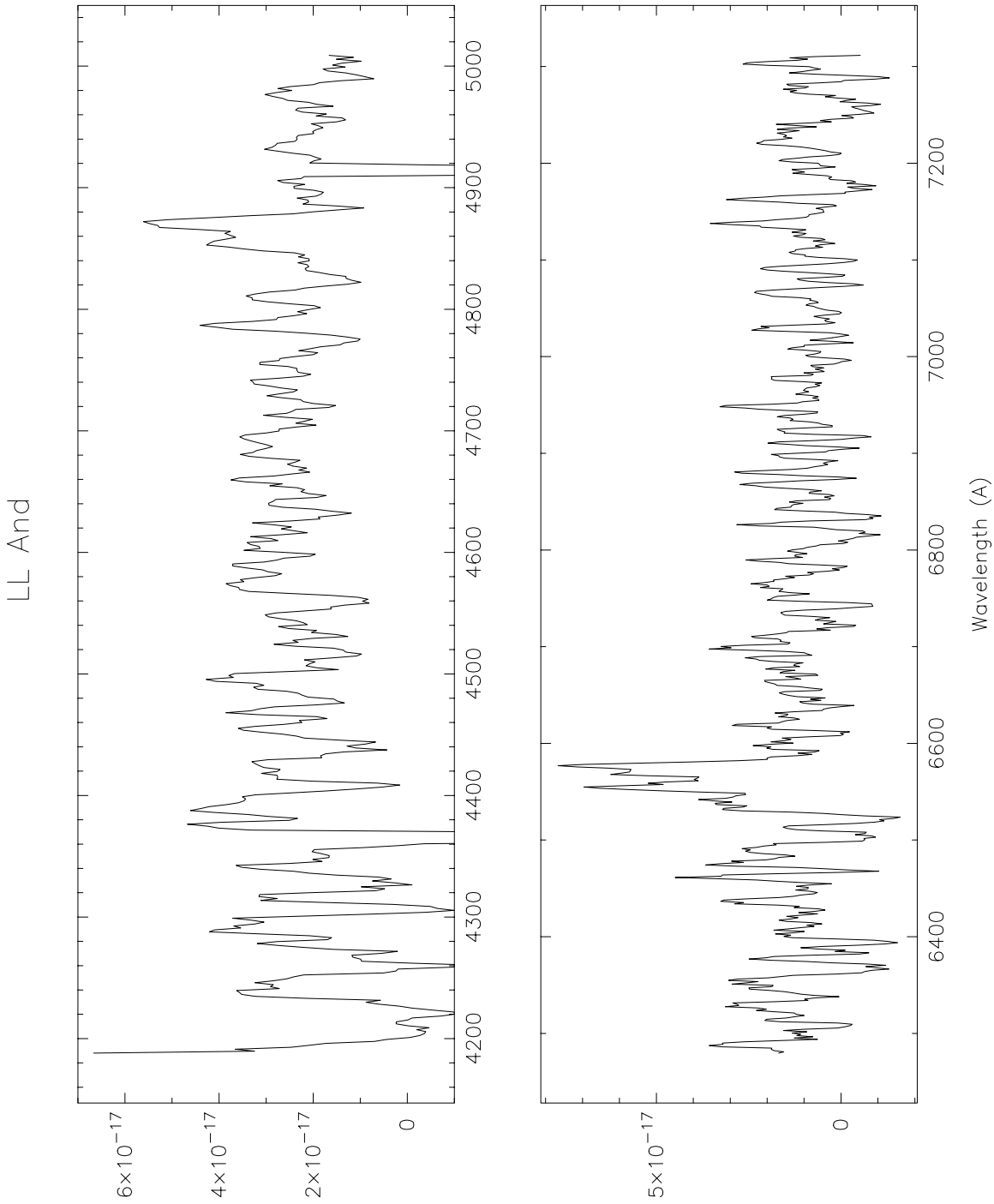
LL And
6×10^-17
4×10^-17
2×10^-17
0
4200
4300
4400
4500
4600
4700
4800
4900
5000
5×10^-17
0
6400
6600
6800
7000
7200
Wavelength (A)

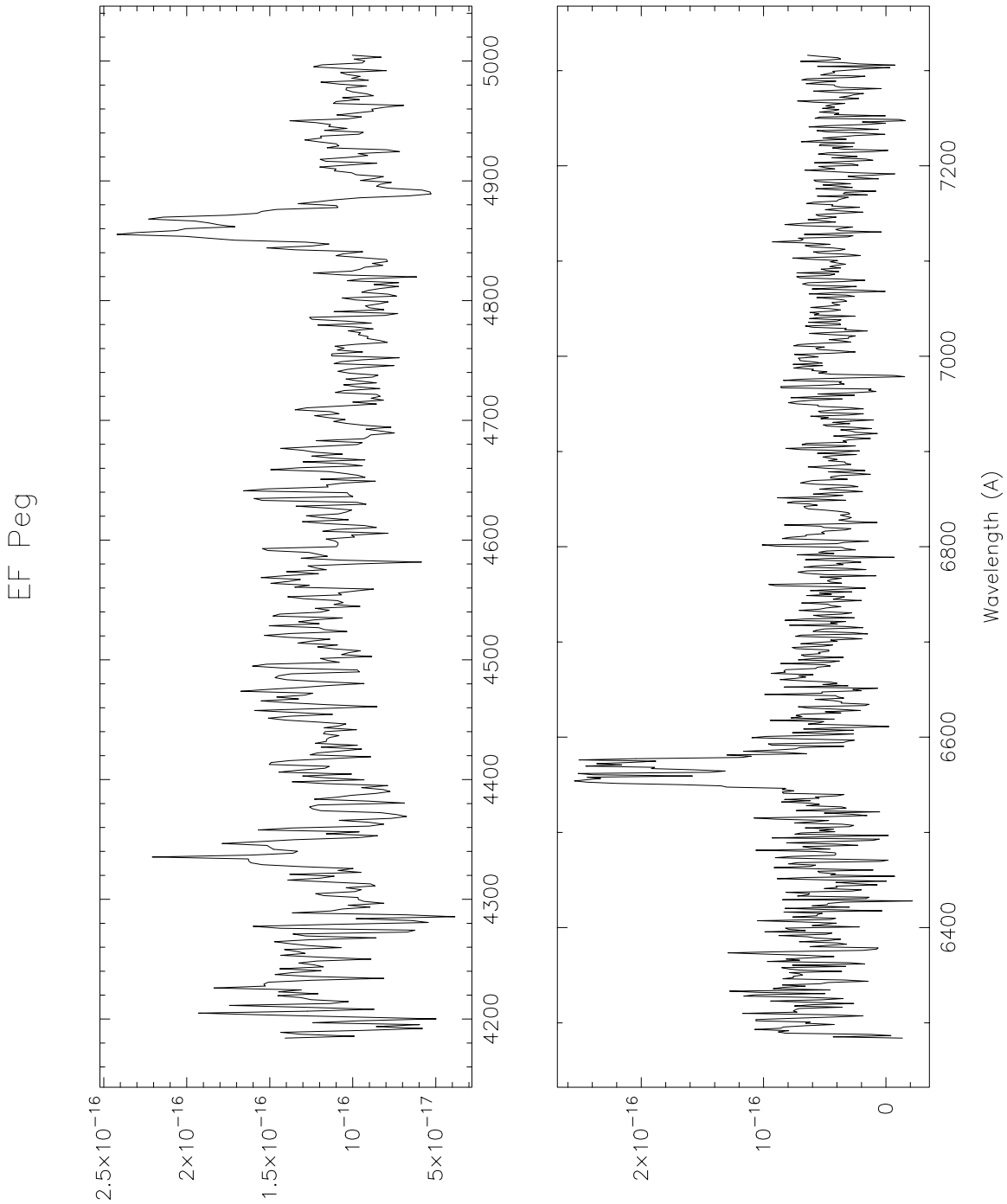
EF Peg
2.5×10⁻¹⁶
2×10⁻¹⁶
1.5×10⁻¹⁶
10⁻¹⁶
5×10⁻¹⁷
4200
4300
4400
4500
4600
4700
4800
4900
5000
2×10⁻¹⁶
10⁻¹⁶
0
6400
6600
6800
7000
7200
Wavelength (A)

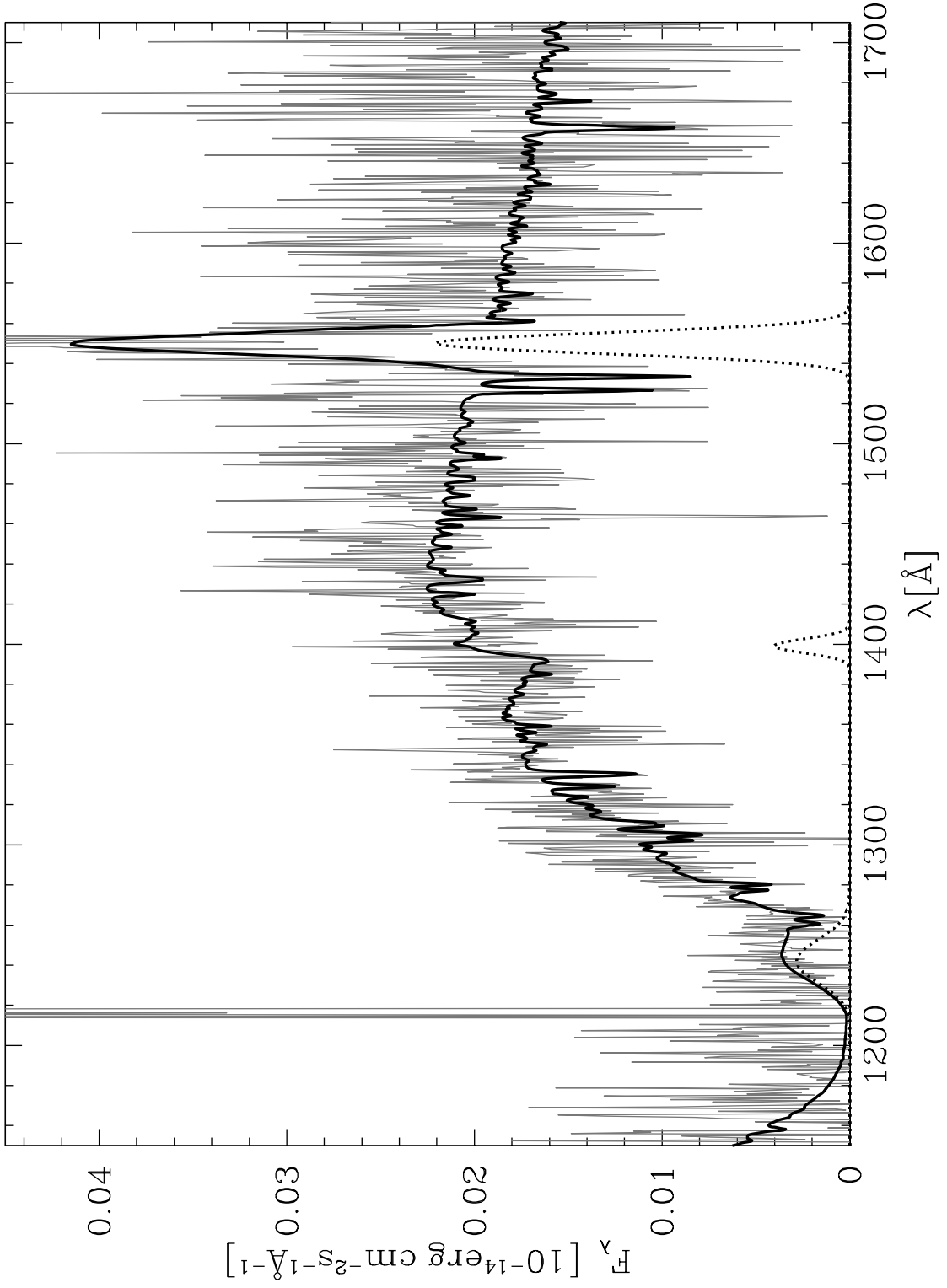
0.04
0.03
0.02
0.01
0
1200
1300
1400
1500
1600
1700
λ[Å]
F_λ [10^{-14}erg cm^{-2}s^{-1}Å^{-1}]

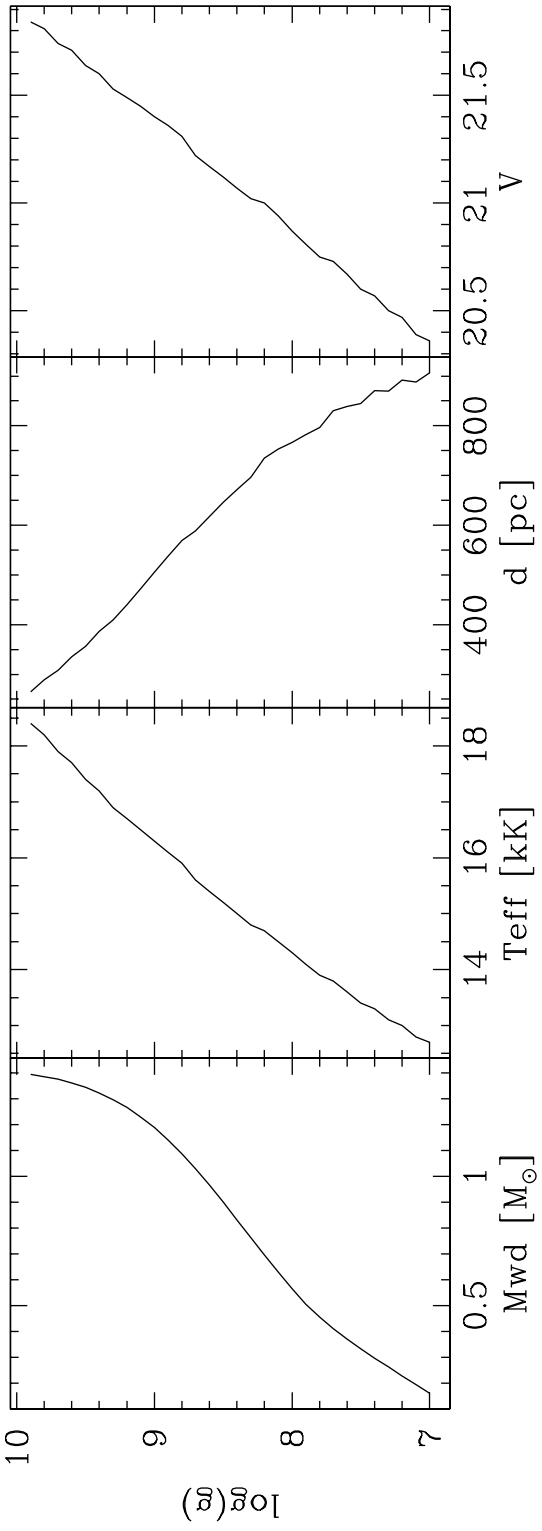
log(g)
10
9
8
7
0.5
1
Mwd [M⊙]
14
16
18
Teff [kK]
400
600
800
d [pc]
20.5
21
21.5
V

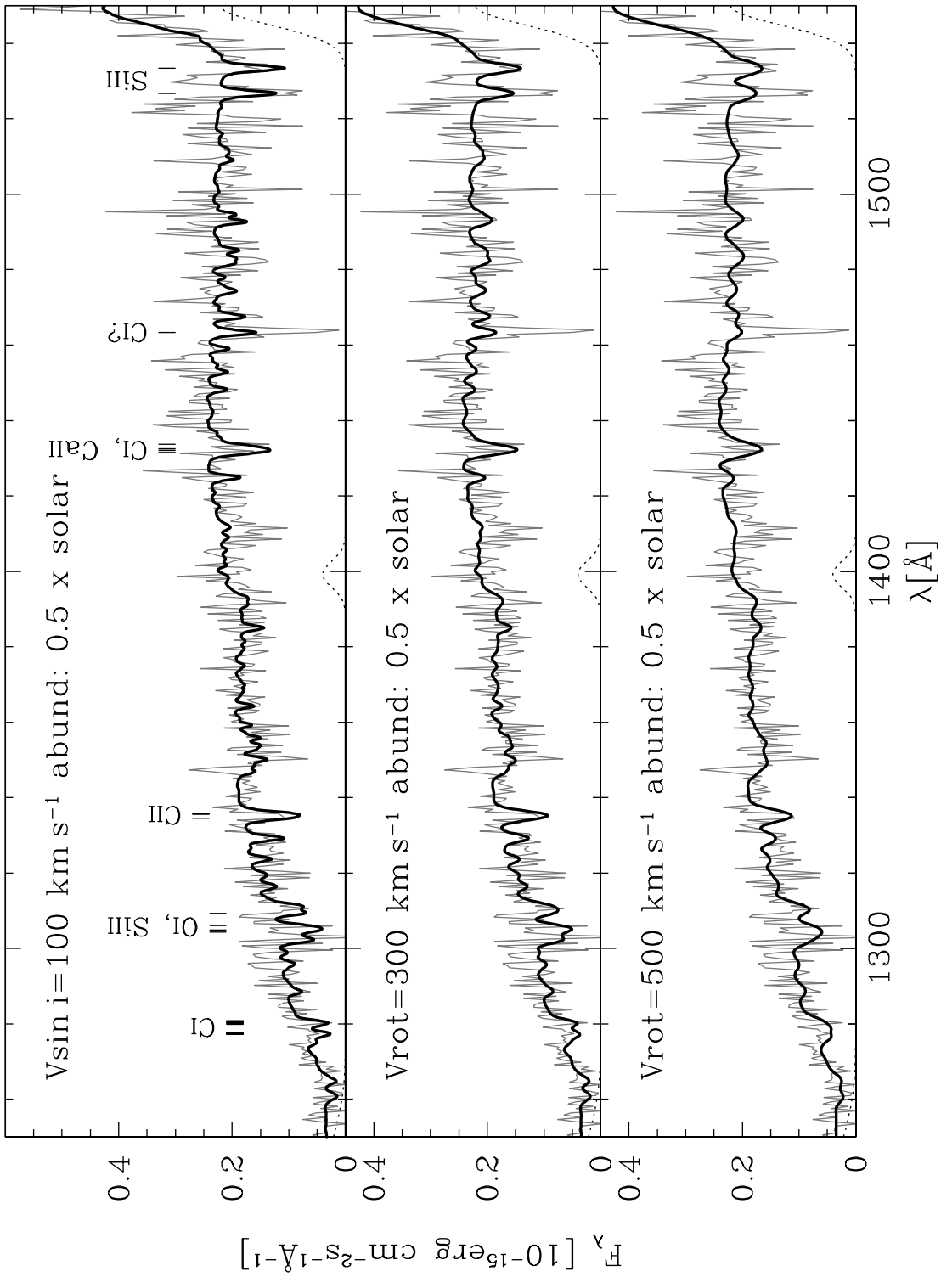
Vsin i=100 km s⁻¹ abund: 0.5 x solar
Vrot=300 km s⁻¹ abund: 0.5 x solar
Vrot=500 km s⁻¹ abund: 0.5 x solar
CI
OI, SiII
CII
CI, CaII
CI?
SiIII
0
0.2
0.4
1300
1400
1500
λ[Å]
Fλ [10⁻¹⁵erg cm⁻²s⁻¹Å⁻¹]

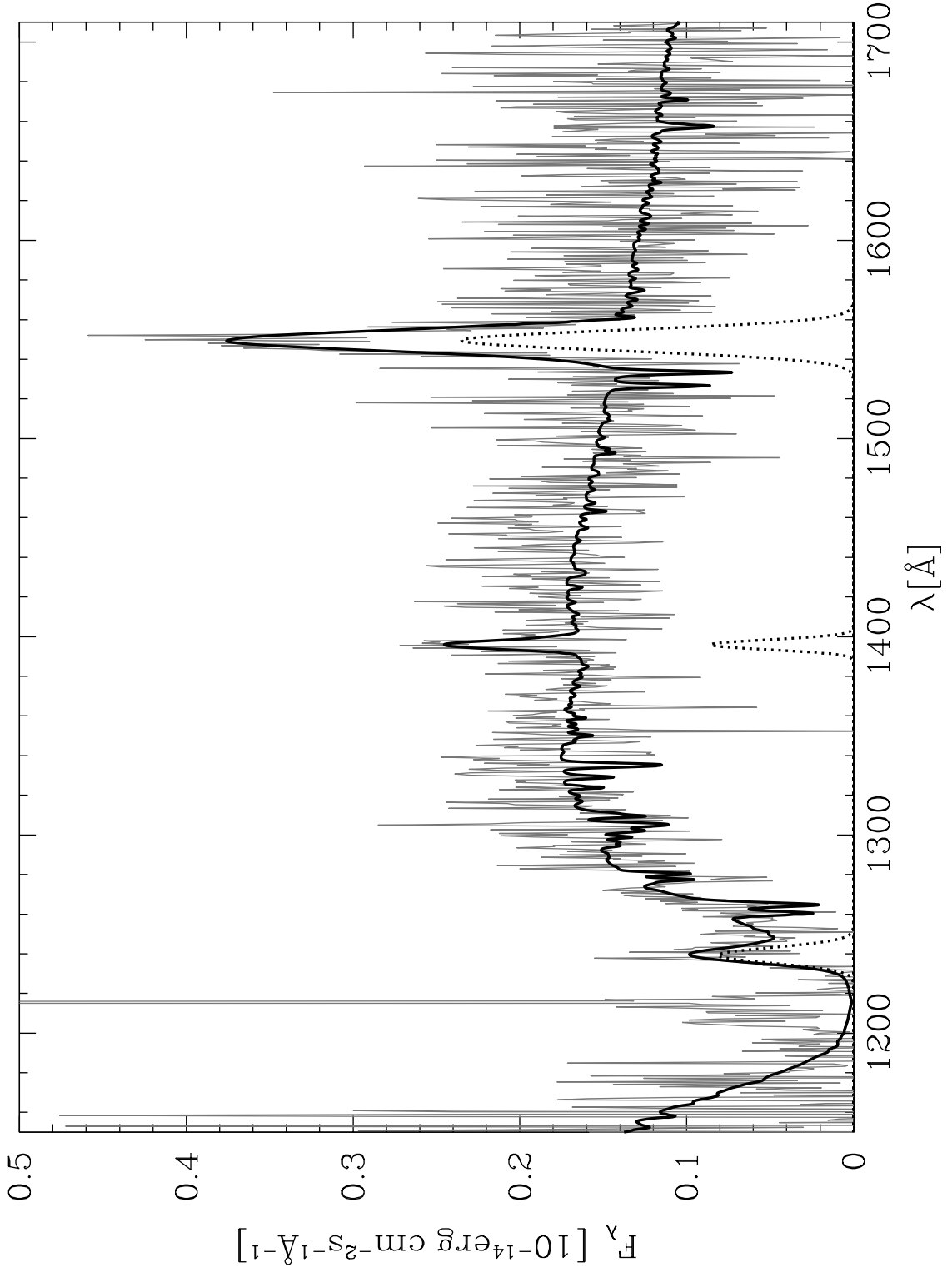
0.5
0.4
0.3
0.2
0.1
0
1200
1300
1400
1500
1600
1700
λ[Å]
F_λ [10^-14 erg cm^-2 s^-1 Å^-1]

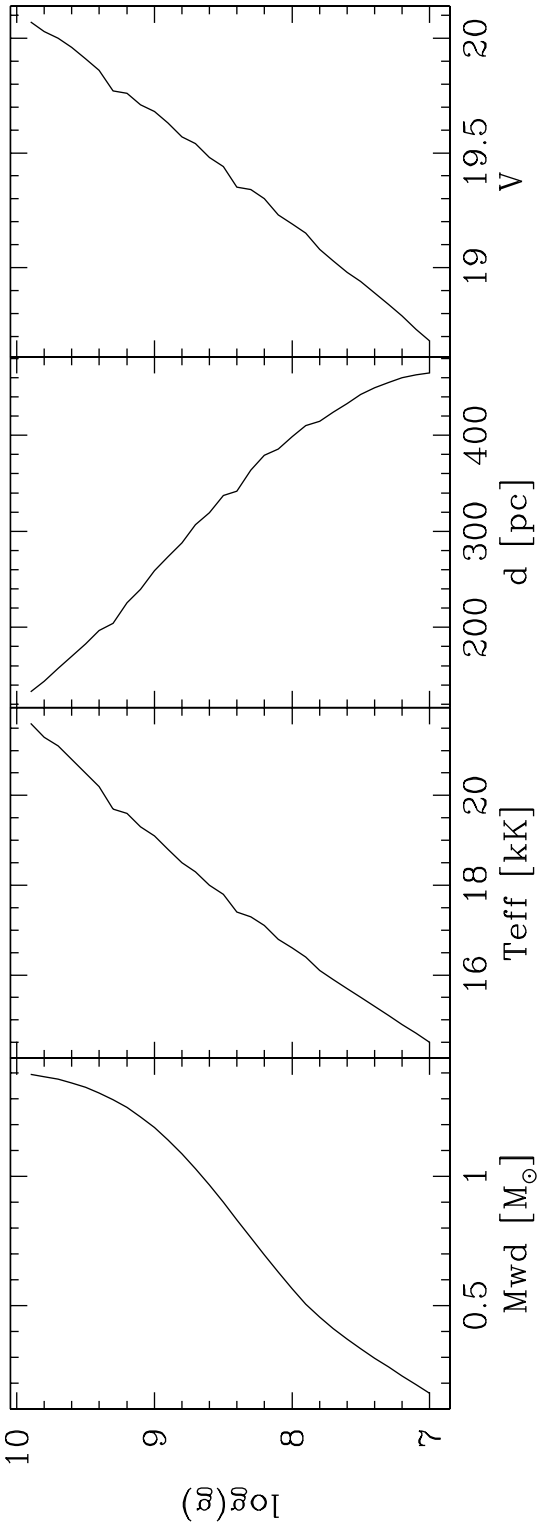
log(g)
10
9
8
7
0.5
1
Mwd [M⊙]
16
18
20
Teff [kK]
200
300
400
d [pc]
19
19.5
20
V

V sin i=100 km s⁻¹ abund: C=0.5 x solar, Rest=0.1 x solar
V sin i=300 km s⁻¹ abund: C=0.5 x solar, Rest=0.1 x solar
V sin i=500 km s⁻¹ abund: C=0.5 x solar, Rest=0.1 x solar
SiII
CI
CI
CI?
1300
1400
1500
λ[Å]
F_λ [10⁻¹⁵erg cm⁻²s⁻¹Å⁻¹]

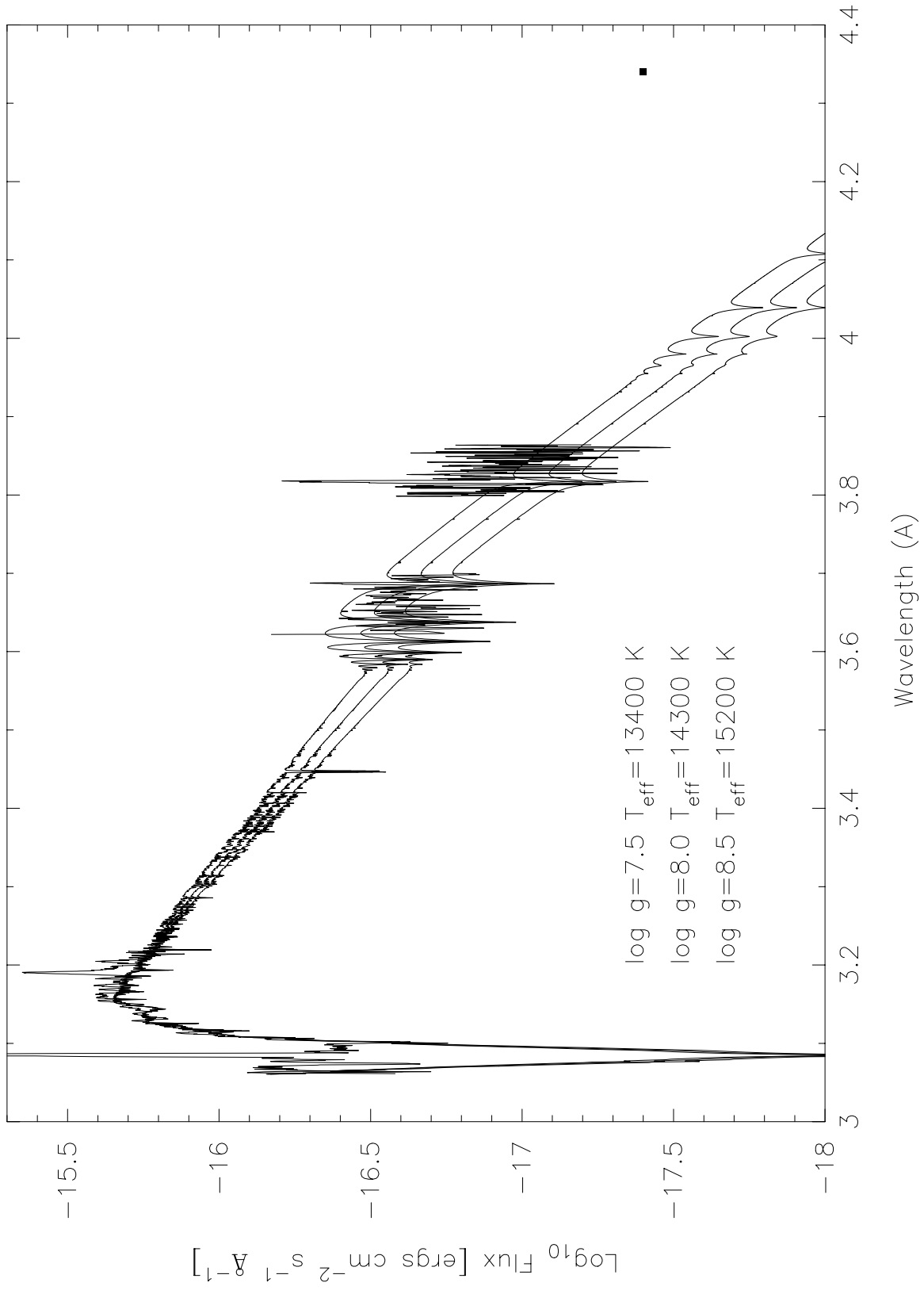
log g=7.5 T_eff=13400 K
log g=8.0 T_eff=14300 K
log g=8.5 T_eff=15200 K
Log10 Flux [ergs cm^-2 s^-1 A^-1]
Wavelength (A)
−15.5
−16
−16.5
−17
−17.5
−18
3
3.2
3.4
3.6
3.8
4
4.2
4.4

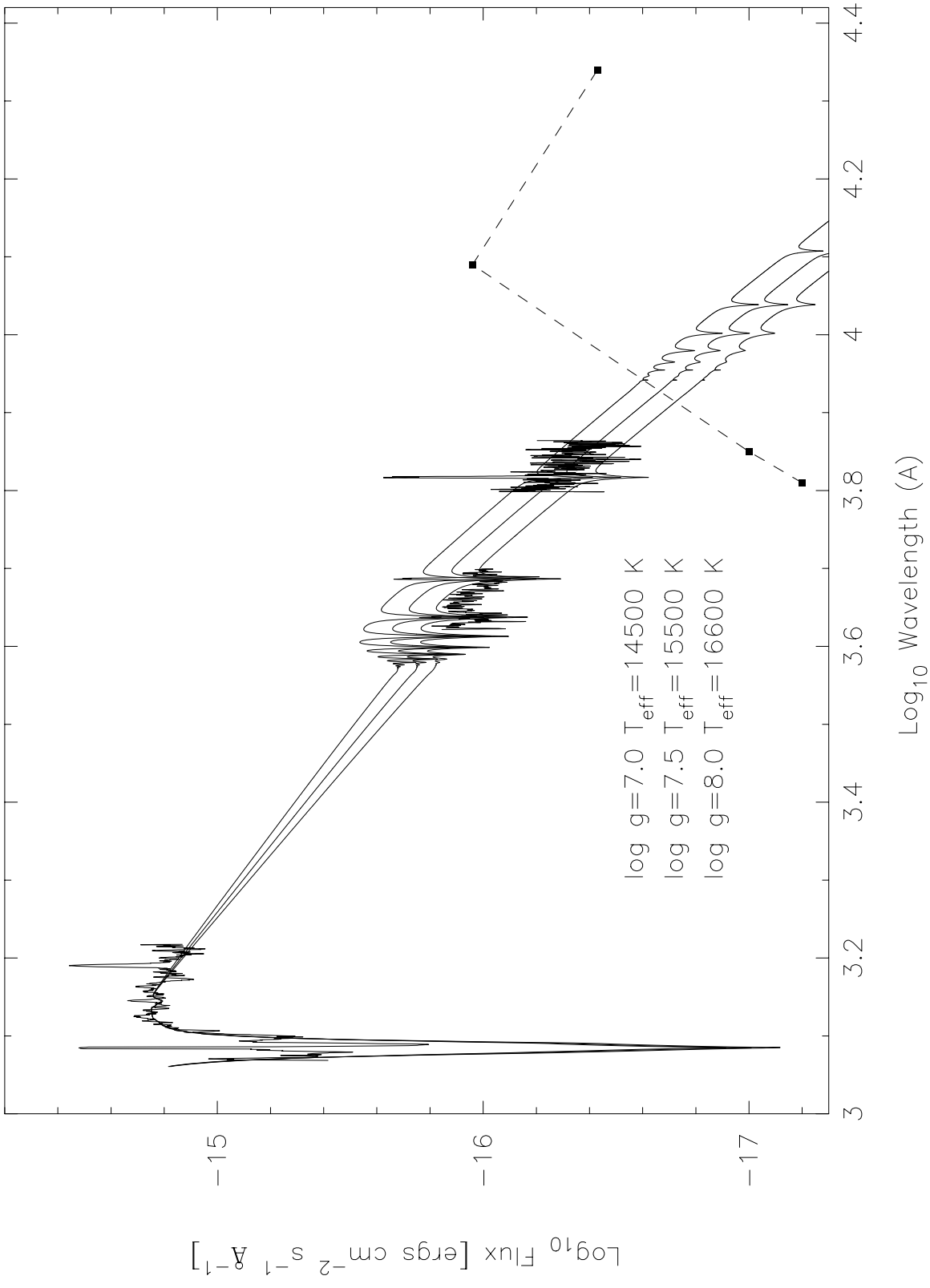
log g=7.0 T_eff=14500 K
log g=7.5 T_eff=15500 K
log g=8.0 T_eff=16600 K
Log10 Wavelength (A)
Log10 Flux [ergs cm-2 s-1 A-1]
3
3.2
3.4
3.6
3.8
4
4.2
4.4
−15
−16
−17